

# Observation of superabsorption by correlated atoms

Daeho Yang, Seung-hoon Oh, Junseok Han, Gibeom Son, Junki Kim,\* Jinuk Kim, and Kyungwon An†  
*Department of Physics and Astronomy & Institute of Applied Physics, Seoul National University, Seoul 08826, Korea*

Emission and absorption of light lie at the heart of light-matter interaction[1–4]. Although the emission and absorption rates are regarded as intrinsic properties of atoms and molecules, various ways to modify these rates have been sought in critical applications such as quantum information processing[5], metrology[6, 7] and light-energy harvesting[8, 9]. One of the promising approaches is to utilize collective behavior of emitters as in superradiance[10]. Although superradiance has been observed in diverse systems[6, 11–16], its conceptual counterpart in absorption has never been realized[17, 18]. Here, we demonstrate superabsorption, enhanced cooperative absorption, by correlated atoms of phase-matched superposition state. By implementing an opposite-phase-interference idea on a superradiant state or equivalently a time-reversal process of superradiance, we realized the superabsorption with its absorption rate much faster than that of the ordinary ground-state absorption. The number of photons completely absorbed for a given time interval was measured to be proportional to the square of the number of atoms. Our approach, breaking the limitation of the conventional absorption, can help weak-signal sensing[4, 19] and advance efficient light-energy harvesting[17, 18] as well as light-matter quantum interfaces.

Correlation among emitters can enhance the radiative decay and make the radiation intensity nonlinearly depend on the number of emitters[10]. Recent technical advances in preparing the emitters with a prescribed correlation made possible to observe enhanced radiation or superradiance immediately without a correlation buildup time. Such controlled superradiance using correlation-prescribed superradiant states has been realized with trapped neutral atoms[6] and ions[13, 14], superconducting qubits[15], layers of x-ray emitting nuclei in solid[20] and flying atoms[16]. Capacity to prepare superradiant states naturally leads us to ponder the long-standing question whether a superradiant state can be engineered to exhibit enhanced absorption in addition to its superradiance.

Absorption is a stimulated coherent process just like stimulated emission and their Einstein B coefficients are the same[21] except for multiplicity factors. A superradiant state, with equal number of ground and excited emitters, should then have the same emission and absorption rates proportional to the square of the number

of atoms in principle. Superabsorption, anticipated enhanced absorption of a superradiant state of correlated emitters, if it exists, would greatly impact light-energy harvesting[17, 18] such as in solar cells and photosynthesis, and advance weak signal sensing and efficient light-matter quantum interfaces[5]. However, superabsorption does not occur in nature under ordinary conditions as evidenced by the absence of its observation so far. For example, in the conventional superradiance by initially fully excited atoms, the atomic correlation and its associated phase are automatically set up in the course of emission and the superradiant state keeps proceeding to the lower states in the Dicke ladder[10] undergoing enhanced emission without absorption. Although the recent theoretical proposals[17, 18] suggest to prevent the superradiant state from going down the Dicke ladder by eliminating the density of states for the downward transition and only allow the upward transition or superabsorption to occur, its experimental realization remains still illusive.

In this work, we have experimentally realized superabsorption for the first time by implementing destructive interference between an input field and the emission amplitude of a superradiant state of correlation-prescribed multiple atoms prepared in a cavity. In the absence of an input field, the superradiant state would generate a coherent-state superradiant field with its phase determined by that of the superradiant state of atoms[16]. Injection of an input field into the cavity with an opposite phase to that of the prospect superradiant field then brings about superabsorption of the input field via destructive interference between two fields. We observed greatly enhanced absorption with the number of absorbed photons scaling as the square of the number of atoms while its rate faster than the ordinary ground-state absorption.

To understand how our superabsorption works, it is worth noting first that ordinary ground-state absorption can be interpreted as an interference between an input field and the emitted field by the weakly excited atoms. As illustrated in Fig. 1a, a small dipole moment excited by an input field emits an opposite-phase field with a small amplitude, which then destructively interferes with the input to diminish it, resulting in the familiar ground-state absorption. This picture can be extended to a superradiant state, an  $N$ -atom symmetric state initially prepared in the equator in the  $N$ -atom Bloch sphere, which can be defined in terms of the collective spin operator  $\hat{J}_\mu = \frac{1}{2} \sum_{i=1}^N \hat{\sigma}_i^\mu$  with  $\mu = x, y, z$ . Because of a large dipole moment associated with the superradiant state, it would emit a large-amplitude field, which can interfere destructively with an input field if the input has an opposite phase to the superradiant field as in Fig. 1b. Such destructive interference

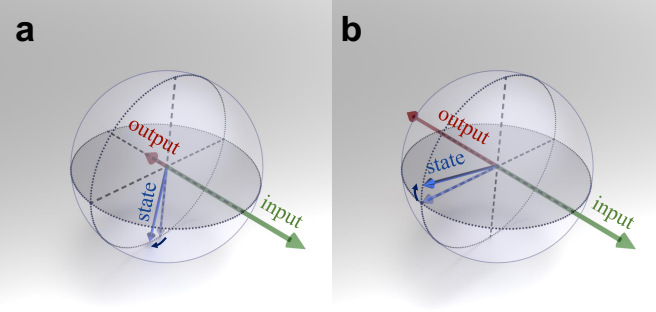


FIG. 1. **Superabsorption as destructive interference.** Bloch sphere with a Bloch vector corresponding to an  $N$ -atom state, an input field and the output(emitted) field by the atomic dipole. **a**, Atoms are initially in the ground state. **b**, Atoms are initially in a superradiant state. Destructive interference between the input and emitted fields can lead to enhanced absorption or superabsorption. The reduced amount of light energy by the destructive interference is coherently transferred to the internal energy of the atoms.

can bring about much stronger absorption or the superabsorption we seek. For an input field with an arbitrary phase, conversely, the phase of superradiant state can be adjusted to meet the opposite-phase requirement.

Alternatively, we can envisage our superabsorption as a time-reversed process of the emission by the superradiant state corresponding to a Bloch vector in the equator of the  $N$ -atom Bloch sphere. In the absence of an input field, the emission process of the  $N$ -atom Bloch vector in a cavity can be described by

$$\hat{U}(t) |\Psi\rangle_a |0\rangle_f = |\Psi'\rangle_a |\alpha\rangle_f, \quad (1)$$

where  $\hat{U}(t) \equiv e^{-i\hat{H}t/\hbar}$  denotes the time-evolution operator of the Tavis-Cummings Hamiltonian  $\hat{H} = \hbar g \sum_{i=1}^N (\hat{a}^\dagger \hat{\sigma}_i + \hat{a} \hat{\sigma}_i^\dagger)$  with  $\hat{a}(\hat{a}^\dagger)$  the annihilation(creation) operator for the cavity field and  $\hat{\sigma}_i(\hat{\sigma}_i^\dagger)$  the lowering(raising) operator for the  $i$ th atom,  $|0\rangle_f$  denotes a photonic vacuum state,  $|\alpha\rangle_f$  represents a photonic coherent state with an amplitude  $\alpha$  and  $|\Psi'\rangle_a$  is the resulting atomic state by the time evolution. Equation (1) describes a superradiance process, where the average photon number of the coherent state  $|\alpha\rangle_f$  is proportional to  $N^2$ [16]. By introducing a field-phase-flipping operator  $\hat{R}_\pi$  corresponding to  $\pi$ -rotation in the field phase space and by utilizing the relation  $\hat{R}_\pi \hat{U}(t) \hat{R}_\pi^\dagger = \hat{U}(-t)$ , one can then show (see Methods for details)

$$\hat{U}(t) |\Psi'\rangle_a |-\alpha\rangle_f = |\Psi\rangle_a |0\rangle_f. \quad (2)$$

What it means is as follows. By preparing the cavity with an initial state  $|-\alpha\rangle_f$ , we achieve the time reversal of the superradiance process in Eq. (1). The atomic state returns to the initial state and the cavity field is completely absorbed to a vacuum state with the absorbed number

of photons proportional to  $N^2$ . This time-reversal interpretation is perfectly consistent with the aforementioned destructive-interference picture of superabsorption: the input field  $|-\alpha\rangle_f$  required for the time reversal process destructively interferes with the prospect superradiant output field  $|\alpha\rangle_f$ .

Let us now consider our experiment. A beam of two-level atoms ( $^1S_0 \leftrightarrow ^3P_1$  transition at  $\lambda=791\text{nm}$  of barium 138) traveling in  $y$  direction in Fig. 2a goes through a nanohole-array aperture in a checkerboard pattern with a period of  $\lambda$ . Just behind the nanohole array, the atoms are excited by a pump laser propagating in  $x$  direction with a pulse area of  $\Theta$  and then enter a high-finesse Fabry-Pérot cavity. By the nanohole array, the atomic vertical ( $x$ ) position is localized at  $\pi$ -different equiphase planes of the pump laser and its horizontal ( $z$ ) position localized at one of the cavity anti-nodes (Fig. 2b). With both the atom-cavity coupling and the pump laser phase alternating their signs with a period of  $\lambda/2$ , every atom is then excited to a superposition state of the ground and excited states with the same atom-cavity relative phase. Under this condition, the atomic state can be written as  $|\Psi\rangle_a = \prod_{k=1}^N [\cos(\Theta/2) |g\rangle_k + \exp(-i\phi_0) \sin(\Theta/2) |e\rangle_k]$ , where  $N$  is the number of atoms in the cavity,  $g(e)$  stands for the ground(excited) state of the atom and  $\phi_0$  is the common atom-cavity relative phase. Our experiment corresponds to a strong coupling regime for single atoms with  $(\gamma_a, \gamma_c, \bar{g}) = 2\pi \times (25, 131, 256)\text{kHz}$ , where  $\gamma_a(\gamma_c)$  is the atomic(cavity-field) half linewidth and  $\bar{g}$  is the spatial-averaged atom-cavity coupling. Due to the strong coupling and a short atom-cavity interaction time  $\tau \approx 100$  ns, the spontaneous emission into free space and thus the decoherence of the atomic state can be neglected during  $\tau$ .

Contrary to the randomly distributed atomic dipoles, every dipole moment  $\mathbf{p}$  of our atomic state is the same with an identical phase and thus the total dipole moment in the cavity behaves like a macro dipole,  $N\mathbf{p}$ . Although each dipole resides in the cavity only for a short time  $\tau$ , since the dipole moment of a newly entering atom is perfectly in phase with the preceding ones, coherence is maintained among the dipoles with different entering times. The sustained coherence among entering and exiting dipoles allows us to simplify our system as a macro dipole  $N\mathbf{p}$  stationary in the cavity under the condition that the atomic state does not change much during the time interval under consideration within the coherence time, so the description by Eqs. (1) and (2) can be applied to our experiment. As a supporting data, enhanced radiation or superradiance by these  $N$  atoms is observed(Fig. 2c) without any input field. Due to the coherence among the dipoles, the superposition state( $\Theta = \pi/2$ ) emits more photons than the fully excited state( $\Theta = \pi$ ) when the holes of the aperture are centered at the cavity anti-nodes( $\Delta z = 0$ ). Note that *uncorrelated* superposition-state( $\Theta = \pi/2$ ) atoms with random phases would emit much less than the fully excited atoms because of zero population inversion.

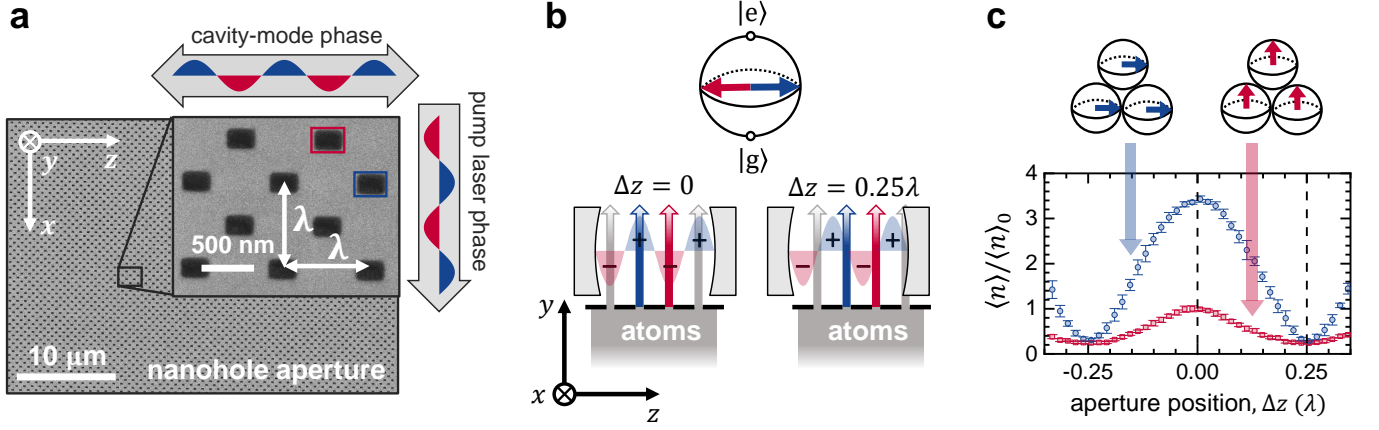


**FIG. 2. Experimental scheme and state preparation with a nanohole array.** **a**, Images of the nanohole-array aperture captured with a scanning electron microscope. Two-level atoms in a beam traveling in  $y$  direction are excited by a pump laser propagating in  $x$  direction to a superposition state after filtered by the nanohole array aperture. The state-prepared atoms interact with the cavity mode, whose axis lies in  $z$  direction, for a short time and emit or absorb photons in the cavity. Period of the nanohole array matches the transition wavelength of the two-level atom ( $\lambda = 791$  nm). The total array size is  $50\lambda \times 50\lambda$ . The single(double)-headed arrow indicates the traveling(standing) wave nature of the pump(cavity) field with the sinusoidal oscillation depicting the phase variation. **b**, Bloch sphere of the atomic dipoles passing through the red(blue)-marked hole is associated with a pump laser phase of  $0(\pi)$ . Since the atom-cavity coupling of the atoms going through the red-marked hole is opposite to that of the blue-marked hole, these two group of atoms experience the same atom-cavity relative phase. **c**, Changing the aperture position,  $\Delta z$ , along the cavity axis gives position-dependent radiation induced by the anti-node/node structure of the cavity. Experimentally-observed radiation intensity is shown in a normalized average photon number,  $\langle n \rangle / \langle n \rangle_0$ , where  $\langle n \rangle_0$  is the maximum number of photons that would be generated by a fully excited atoms (red Bloch vector). Superposition state (blue Bloch vector) radiates much more than the fully excited state due to the correlation among dipoles. The number of atoms in the cavity is  $\langle N \rangle = 2.7$  for both cases.

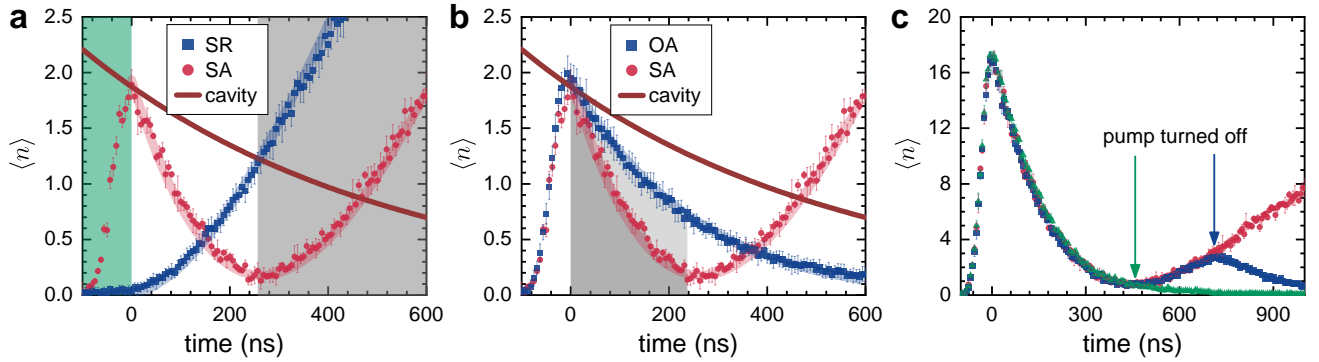


**FIG. 3. Time-dependent intracavity photon number by superradiance, superabsorption, and ordinary absorption.** **a**, The superradiant state emits photons (blue dots), starting from  $\langle n \rangle = 0$  and grows quadratically in time due to the cavity-mediated atomic coherence. If we initially prepare an opposite-phase field (green shaded area) in the cavity, the superradiant state absorbs photons (red points in the unshaded area) instead of emitting photons. After fully absorbing the photons, the superradiant state starts to radiate (gray shaded area). The absorbing and radiating parts of the curve are nearly symmetric. Small asymmetry is due to the cavity decay (brown curve). **b**, The superabsorption (red dots) of the superradiant state gives a much faster absorption than the ordinary absorption (blue points) of the ground state of atoms. The number of atoms in the cavity is the same for both cases ( $\langle N \rangle \approx 6.8$ ). **c**, For complete superabsorption, the pump laser can be turned off to suppress the subsequent superradiance. Thick shaded curves in **a** and **b** represent the theoretically calculated  $\langle n \rangle$  with no adjustable parameters.

In order to demonstrate the aforementioned time-reversal relation between the superradiance and the superabsorption, we observed both phenomena, radiation and absorption process of the superradiant state in a time-dependent manner (Fig. 3a). With the cavity initially

empty, we let the superradiant-state atoms go through the cavity and emit photons. During the photon buildup, the sustained coherence among the successively entering atomic dipoles makes the photon number increase quadratically in time. It is because the amplitude of the

electric field generated by the constant macro dipole increases linearly in time in the slowly varying envelop approximation. Specifically, the mean number of photons is given by  $\langle n \rangle \simeq |\rho_{eg} N g t|^2$  (see Supplementary Note 1 for the derivation). However, if we initially prepare the cavity with the coherent state  $|\alpha\rangle_f$ , the injected superradiant-state atoms absorb the photons in the cavity instead of emitting photons, undergoing a time-reversed process of superradiance. After fully absorbing photons in the cavity, the superradiant state starts to radiate again because there are no photons to absorb – or no input field to interfere destructively with (see the grey-shaded region in Fig. 3a and Eq. (5) in Methods). The temporal profile of the radiation and that of the absorption seem symmetric except for a mild imbalance due to the cavity decay.

In the superabsorption, the input field can be completely absorbed by the atoms at a finite time given by  $t_0 = \frac{\sqrt{n_0}}{|\rho_{eg}| N g}$  for a given initial photon number  $n_0$ . In contrast, such complete absorption cannot be achieved in a finite time in the ordinary absorption exhibiting an exponential decay of the input field. In the superabsorption data of Fig. 3, a small number of photons ( $\langle n \rangle \sim 0.2$ ) remained unabsorbed due to experimental imperfections such as incomplete phase matching between the input field and the dipoles, the phase variation among dipoles (due to the finite hole size), and atomic spontaneous emission. The superradiant emission commencing after the superabsorption ends may seem an obstacle in practical applications. However, it can be easily suppressed by turning off the pump laser preparing the atoms in the superposition state as demonstrated in Fig. 3c.

For the enhanced absorption by the superradiant state atoms to be called “super” absorption, the absorption rate of the superradiant state should be much faster than that of the ground state. In Fig. 3b, the superradiant state atoms clearly give faster absorption than the ground state atoms. Since a part of photons leaks out due to the cavity decay, for a fair comparison we define the absorption ratio as the number of *absorbed* photons for a given time interval  $t_{ab} \leq t_0$  to the total number of photons initially prepared in the cavity. Assuming the cavity decay follows the Lindblad equation, we can calculate the number of cavity-decayed photons by numerically integrating the expression  $\Gamma_c \int_0^{t_{ab}} \langle n(t) \rangle dt$  (the integral corresponding to the gray shaded areas in Fig. 3b). Taking the numbers of cavity-decayed photons into account, we obtain the absorption ratio of 75% for the superabsorption and 37% for the ordinary absorption. Simple algebra in Supplementary Note 2 shows we need 3.4 times more atoms in the ordinary absorption in order to achieve the same absorption ratio as the superabsorption. Furthermore, it is shown in Supplementary Note 3 that the effective optical depth – an equivalent free-space optical depth – for superabsorption is larger than that of the ordinary absorption by a factor proportional to  $N$ .

One of the most distinctive features of superradiance is its nonlinear scaling of radiation intensity on the atom

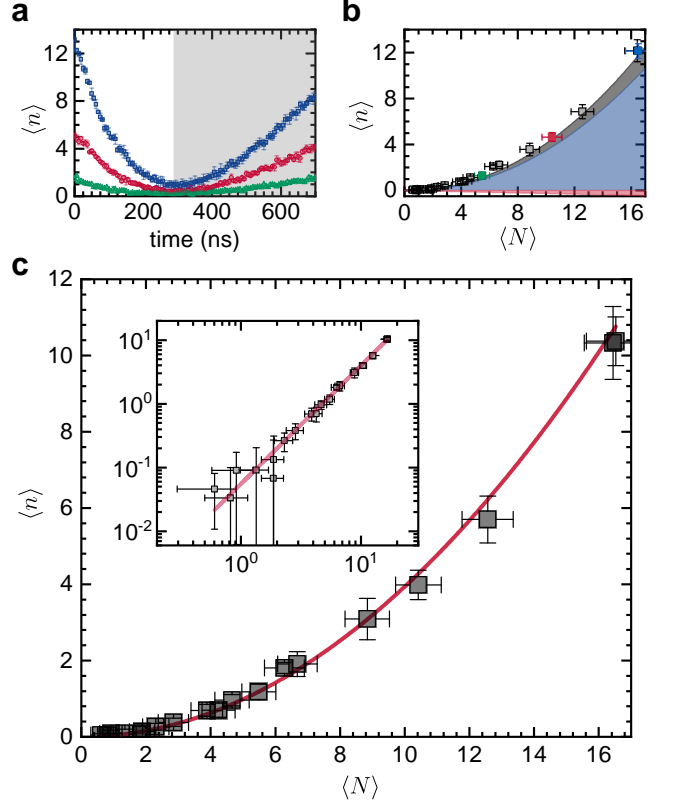


**FIG. 4. Quadratic dependence of superabsorption on atom number.** **a**, Selected temporal profiles of superabsorption process. Because there exists a clear absorption-emission turning point (the border of the shaded area), it is possible to evaluate the maximum number of photons that can be completely absorbed in a fixed time interval  $t_0 (=280\text{ns})$  for a given number of atoms in the cavity. If the number of photons is less than this maximum number, complete absorption takes place before  $t_0$ . If the number of photons larger, absorption becomes incomplete by  $t_0$ . **b**, The reduced number of photons for a time interval from  $t = 0$  to  $280\text{ns}$  as in **a** is plotted for different numbers of atoms. Each colored point (green, red, blue) corresponds to the colored temporal profile in **a**. The upper gray-shaded area indicates the theoretically expected photon number reduction from the cavity decay while the lower red-shaded area indicates the increase by the spontaneous emission. The absorption by the correlated dipoles then corresponds to the sum of the blue- and the red-shaded areas. **c**, The absorbed number of photons obtained in **b** is plotted as a function of the mean number  $\langle N \rangle$  of atoms in the cavity. The results are well fit by  $\langle N \rangle^q$  (red curve) with  $q = 1.86 \pm 0.03$ . The inset shows a linear fit in the log-log plot.

number, that is, the maximum number of emitted photons in a fixed time interval is proportional to  $\langle N \rangle^2$ . Likewise, we can consider nonlinear scaling of the absorbed photons in superabsorption (Fig. 4). We measured the maximum number of photons that can be completely absorbed in a fixed time interval as a function of the number of atoms (Fig. 4a). Note that in the actual experiment the photon number is reduced by both the cavity decay and the absorption by the dipoles but increased by the spon-

taneous emission of the atoms. Their individual contributions calculated from the theory are indicated in Fig. 4b. The number of absorbed photons is then obtained by subtracting the portion by the cavity decay from the observed number of reduced photons and adding the portion from the spontaneous emission to the remaining number of photons. The resulting number of purely absorbed photons by the correlated atoms are plotted in the log-log scale in Fig. 4c. The result can be well fit by the expression  $\langle n \rangle \propto \langle N \rangle^q$  with  $q = 1.86 \pm 0.03$ . The small discrepancies from  $\langle N \rangle^2$  can be explained by the aforementioned experimental imperfections.

It is noteworthy that in our destructive-interference picture of superabsorption as in Fig. 1 the input and output fields do not need to be in a cavity. A cavity just makes the atom-field interactions prolonged and enhanced. Based on this consideration, we expect that superabsorption can also be possible by employing atoms in a superposition state interacting with a tightly focused single-pass input field.

The realization of superabsorption not only deepens our understandings on the cooperative light-matter interactions but also provides new opportunities in the study of fast and efficient absorption[8, 9, 22, 23], light-energy harvesting[17, 18], and weak-signal sensing[4, 19]. One of the advantages of enhanced absorption by manipulating the atomic internal state lies in the way the energy is stored. Since every absorbed photon is coherently stored in an atomic internal state, the enhanced atom-photon coupling from the collective interaction can be utilized in coherence-critical applications such as quantum memory[24] and quantum interfaces[5, 25].

## METHODS

**Nanohole-array aperture.** The nanohole-array aperture was fabricated by using the focused ion beam technique on a 10nm-thick silicon nitride membrane mounted on a 200 $\mu$ m-thick silicon frame. The individual hole size measured with a scanning-electron microscope is  $0.35\lambda \times 0.24\lambda$  ( $\lambda=791$ nm). The horizontal spread of the atomic distribution by the finite hole size has an effect of averaging the atom-cavity coupling. The resulting variation in  $g$  is  $\Delta g/g = 0.20$ . The vertical spread of the atomic distribution decreases atomic phase purity due to the position dependence of the pump laser phase. The height of the hole was thus intentionally made smaller than the width in order to suppress the fluctuations in atomic phase purity while maintaining an enough atomic flux. The aperture is mounted on a 6-axis stage with an additional piezoelectric transducer(PZT) for precise alignment along the cavity axis. The aperture is coarsely placed at the center of the waist of the cavity mode (vertically and horizontally) by the 6-axis stage and then a feedback loop places the center of each hole at cavity anti-nodes by using the PZT. The average atom-cavity coupling is decreased additionally because the height of

the aperture(40 $\mu$ m) is compatible to the cavity mode waist(43 $\mu$ m), and thus  $\Delta g/g = 0.06$ .

**Measurement procedure.** Since the number of photons in the cavity is usually less than 10, repetitive measurements are required. After measuring superradiance or superabsorption, the pump laser for atomic superposition state preparation is turned off. By turning off the pump laser, we let all photons be removed by both the cavity decay and the ordinary absorption by the injected atoms in the ground state. The period of each measurement is 3.2 $\mu$ s and the pump pulse duty cycle is 0.4 (Fig. 5). The cavity decay reduces the photon number by 96% during the pump-off time and the absorption by atoms reduces it further to a near vacuum state. The pump laser pulses are generated with an acousto-optic modulator(AOM) and the pulse timing is controlled by a field-programmable gate array(FPGA). For acquiring one temporal profile of the average photon number such as in Fig. 3, about 2 million measurement cycles are used to accumulate data.

Figure 5 shows the timing diagram and the schematic of the feedback loop for the input laser phase control. There exist two feedback loops – fast and slow ones. The fast feedback loop is obtained by directly interfering the input and the pump lasers and lessen the noise up to the bandwidth of a few kHz by using an AOM. The slow feedback loop is obtained by measuring the number of photons in the cavity, *e.g.* the superabsorption signal, and then slow drifts (up to tens of Hertz) is compensated by using a PZT-mounted mirror. The slow drifts come from the vertical vibrations of the aperture and the optical path-length drift. The phase of the input laser is modulated at 39.1kHz for 25.6  $\mu$ s or  $8 \times 3.2\mu$ s and held constant for another 8 periods of 3.2 $\mu$ s. The first 25.6 $\mu$ s is used to get a lock-in amplifier signal and the second 25.6 $\mu$ s is used to measure the cavity photon number.

Although it is not noticeable in Fig. 5b, the pump laser is turned on slightly earlier than the input laser in order to compensate a time delay in exciting atoms to a desired state. With a DC magnetic field applied to the direction of the atomic beam path, only  $\pi$  transition( $\Delta m = 0$ ) is on resonance with the cavity and other  $\sigma_{\pm}$  transitions( $\Delta m = \pm 1$ ) are shifted out of resonance by 52 MHz (much larger than the atomic transit time broadening of about 10MHz). In accordance with the  $\pi$  transition, the polarization of the pump laser is set to be along the atom-propagating axis.

**Superabsorption by reversing superradiance in time.** The atom-field interaction in our system is described by the Tavis-Cummings Hamiltonian,

$$H = \hbar g \sum_i^N \left( \hat{a}^\dagger \hat{\sigma}_i + \hat{a} \hat{\sigma}_i^\dagger \right), \quad (3)$$

where  $\hat{a}(\hat{a}^\dagger)$  is the annihilation(creation) operator for the cavity field and  $\hat{\sigma}_i(\hat{\sigma}_i^\dagger)$  is the lowering(raising) operator



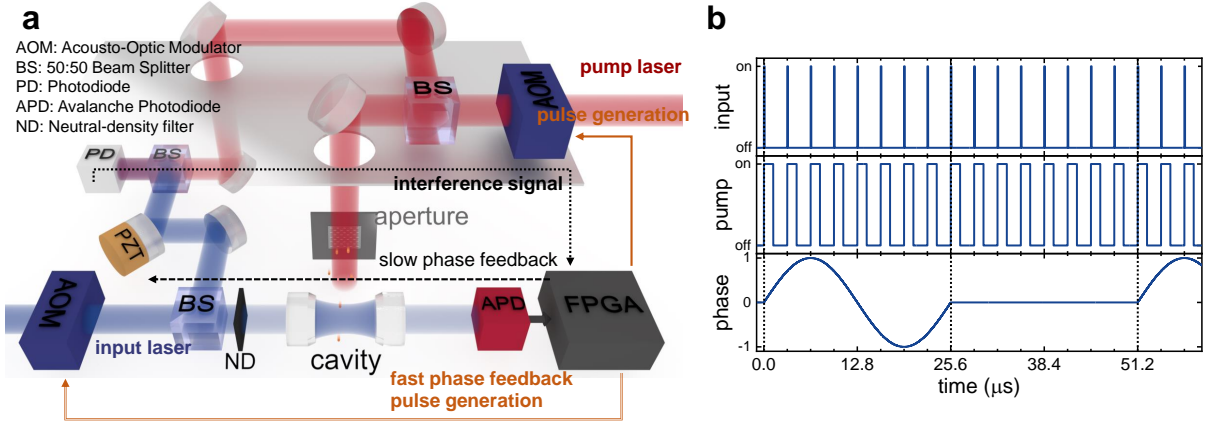


FIG. 5. **Timing diagram for repeated measurements and feedback loop for the input laser phase.** **a**, Feedback loop for the phase control between the pump and the input laser is composed of a direct interferometer and a slow compensator. The direct interferometer captures high frequency noise with the AOM phase modulation and the slow compensator adjusts the mirror-mounted PZT based on the APD(avalanche photodiode) signal. **b**, Time-dependent amplitudes of the input and the pump lasers and the time-dependent phase of the input laser. Laser amplitudes are given as on/off levels and the on-state power is dependent on the experiment. The phase of the input laser is given in an arbitrary unit and the peak-to-peak value used in experiment lies between  $0.25\lambda$  and  $0.5\lambda$ .

for the  $i$ th atom. Superradiance process is then described by the following time evolution operation.

$$\hat{U}(t) |\Psi\rangle_a |0\rangle_f = |\Psi'\rangle_a |\alpha\rangle_f, \quad (4)$$

where  $\hat{U}(t) \equiv e^{-i\hat{H}t/\hbar}$ ,  $|0\rangle_f$  denotes a photonic vacuum state,  $|\alpha\rangle_f$  denotes a photonic coherent state with an amplitude  $\alpha$ , and  $|\Psi'\rangle_a$  denotes the resulting atomic state by the time evolution. We introduce a field-phase flip operator  $\hat{R}_\pi = e^{-i\pi\hat{a}^\dagger\hat{a}}$ , corresponding to  $\pi$ -rotation in the field phase space. The operator  $\hat{R}_\pi$  only acts on the photonic state and satisfies the property,  $\hat{R}_\pi\hat{a}\hat{R}_\pi^\dagger = -\hat{a}$  and similarly  $\hat{R}_\pi\hat{a}^\dagger\hat{R}_\pi^\dagger = -\hat{a}^\dagger$ , and thus  $\hat{R}_\pi^\dagger\hat{U}(t)\hat{R}_\pi = \hat{U}(-t)$ .

The result from simply applying  $\hat{U}(-t)$  on both side of Eq. (4) is the time-reversed process of superradiance,  $\hat{U}(-t)|\Psi'\rangle_a |\alpha\rangle_f = |\Psi\rangle_a |0\rangle_f$ , which is superabsorption. Since direct time-reversing is not experimentally possible, we utilize a phase-flip operation. Let us consider

$$\begin{aligned} \hat{U}(t')|\Psi'\rangle_a |-\alpha\rangle_f &= \hat{U}(t')\hat{R}_\pi^\dagger\hat{R}_\pi|\Psi'\rangle_a |-\alpha\rangle_f \\ &= \hat{U}(t')\hat{R}_\pi^\dagger|\Psi'\rangle_a |\alpha\rangle_f = \hat{R}_\pi^\dagger\hat{U}(-t')|\Psi'\rangle_a |\alpha\rangle_f \\ &= \hat{R}_\pi^\dagger\hat{U}(-t'+t)\hat{U}(-t)|\Psi'\rangle_a |\alpha\rangle_f \\ &= \hat{R}_\pi^\dagger\hat{U}(-t'+t)|\Psi\rangle_a |0\rangle_f = \hat{U}(t'-t)\hat{R}_\pi^\dagger|\Psi\rangle_a |0\rangle_f \\ &= \hat{U}(t'-t)|\Psi\rangle_a |0\rangle_f. \end{aligned} \quad (5)$$

If  $t' = t$ , we completely reverse the superradiance to recover the initial vacuum state. This is superabsorption. If  $t' < t$ , the reversal is not complete. If  $t' > t$ , we then get a normal superradiance process progressing for a time period of  $t' - t$ . Therefore, we can realize time-reversal process of superradiance by preparing the field state as  $|-\alpha\rangle_f$  and by letting the system evolve in an appropriate time.

\* Present address: Department of Electrical and Computer Engineering, Duke University, Durham, North Carolina 27708, USA

† Correspondence to: kwan@phy.snu.ac.kr

- [1] A. L. Schawlow and C. H. Townes, Phys. Rev. **112**, 1940 (1958).
- [2] E. F. Schubert, “Light-emitting diodes,” (2018).
- [3] H. A. Atwater and A. Polman, Nat. Mater. **9**, 205 (2010).
- [4] G. Konstantatos and E. H. Sargent, Nat. Nanotechnol. **5**, 391 (2010).
- [5] K. Hammerer, A. S. Sørensen, and E. S. Polzik, Rev. Mod. Phys. **82**, 1041 (2010).
- [6] M. A. Norcia, M. N. Winchester, J. R. Cline, and J. K. Thompson, Sci. Adv. **2**, e1601231 (2016).
- [7] M. A. Norcia, J. R. Cline, J. A. Muniz, J. M. Robinson, R. B. Hutson, A. Goban, G. E. Marti, J. Ye, and J. K. Thompson, Phys. Rev. X **8**, 021036 (2018).
- [8] A. Olaya-Castro, C. F. Lee, F. F. Olsen, and N. F. Johnson, Phys. Rev. B **78**, 085115 (2008).
- [9] G. L. Celardo, P. Poli, L. Lussardi, and F. Borgonovi, Phys. Rev. B **90**, 085142 (2014).
- [10] R. H. Dicke, Phys. Rev. **93**, 99 (1954).
- [11] N. Skribanowitz, I. Herman, J. MacGillivray, and M. Feld, Phys. Rev. Lett. **30**, 309 (1973).
- [12] M. Gross and S. Haroche, Phys. Rep. **93**, 301 (1982).
- [13] R. DeVoe and R. Brewer, Phys. Rev. Lett. **76**, 2049 (1996).
- [14] B. Casabone, K. Friebe, B. Brandstätter, K. Schüppert, R. Blatt, and T. Northup, Phys. Rev. Lett. **114**, 023602 (2015).
- [15] J. Mlynek, A. Abdumalikov, C. Eichler, and A. Wallraff, Nat. Commun. **5**, 5186 (2014).
- [16] J. Kim, D. Yang, S.-h. Oh, and K. An, Science **359**, 662 (2018).
- [17] K. Higgins, S. Benjamin, T. Stace, G. Milburn, B. W. Lovett, and E. Gauger, Nat. Commun. **5**, 4705 (2014).
- [18] W. M. Brown and E. M. Gauger, arXiv preprint

arXiv:1803.08036 (2018).

- [19] W. Chen, Ş. K. Özdemir, G. Zhao, J. Wiersig, and L. Yang, *Nature* **548**, 192 (2017).
- [20] A. I. Chumakov, A. Q. Baron, I. Sergueev, C. Strohm, O. Leupold, Y. Shvydko, G. V. Smirnov, R. Rüffer, Y. Inubushi, M. Yabashi, *et al.*, *Nat. Phys.* **14**, 261 (2018).
- [21] A. Einstein, *Verh. Deutsch. Phys. Gesell.* **18**, 318 (1916).
- [22] M. O. Scully, *Phys. Rev. Lett.* **104**, 207701 (2010).
- [23] K. D. Higgins, B. W. Lovett, and E. Gauger, *J. Phys. Chem. C* **121**, 20714 (2017).
- [24] B. Julsgaard, J. Sherson, J. I. Cirac, J. Fiurášek, and E. S. Polzik, *Nature* **432**, 482 (2004).
- [25] L. Lamata, D. Leibbrandt, I. Chuang, J. I. Cirac, M. Lukin, V. Vuletić, and S. Yelin, *Phys. Rev. Lett.* **107**, 030501 (2011).

## Acknowledgements

This work was supported by Samsung Science and Technology Foundation (Project No. SSTF-BA1502-05) and the Ministry of Science and ICT of Korea under ITRC program (Grand No. IITP-2019-2018-0-01402).

## Author Contributions

D.Y. and K.A. conceived the experiment. D.Y., S.O., J.H. and G.S performed the experiment. D.Y. analyzed the data and carried out theoretical investigations. K.A. supervised overall experimental and theoretical works. D.Y. and K.A. wrote the manuscript. All authors participated in discussions.

## Additional Information

**Competing Financial Interests** The authors declare no competing financial interests.